

INTERNATIONAL SOCIETY FOR SOIL MECHANICS AND GEOTECHNICAL ENGINEERING



This paper was downloaded from the Online Library of the International Society for Soil Mechanics and Geotechnical Engineering (ISSMGE). The library is available here:

<https://www.issmge.org/publications/online-library>

This is an open-access database that archives thousands of papers published under the Auspices of the ISSMGE and maintained by the Innovation and Development Committee of ISSMGE.

The effect of dynamic compaction on dry granular soils

L'effet du compactage dynamique sur les sols granuleux secs

M.T.H.J.H.SMITS, Geotechnical Engineer, Fugro Geotechniek B.V., Leidschendam, Netherlands
L.DE QUELERIJ, Manager of Engineering, Fugro Geotechniek B.V., Leidschendam, Netherlands

SYNOPSIS

Dynamic compaction is the improvement of the mechanical characteristics of a soil by dropping heavy pounders from a height. This method has been in use for some time for treatment of saturated clays and other less permeable soils, but recently it was successfully applied on dry granular soils as well. This paper presents a new one-dimensional model which adequately describes the compaction mechanism. This model, which was validated by field test results, is a powerful tool for the development of dynamic compaction techniques for use on dry granular soils.

1 INTRODUCTION

The principles of dynamic compaction on saturated soils are described by a number of authors. A full description of the method, including some field results, was given by Ménard and Broise (1975). Various case histories have been presented by Ménard (1974). Classical consolidation theory is inadequate to describe dynamic compaction in saturated soils, because it can not explain the very fast consolidation of clayey soils under heavy tamping. One of the factors causing the rapid consolidation is that the permeability during dynamic loading increases, thus accelerating the consolidation process. This increase in permeability is caused by the creation of vertical fissures, by the decrease in effective stress and perhaps by the increase in cross-sectional area of the capillary channels as a result of the transformation of absorbed water into free water through the shockwave. Another factor causing fast consolidation is that the compressibility of this type of soil is large due to the presence of gas in the form of microbubbles.

In dry soils, none of the above mentioned effects will occur. Compaction here is merely the result of exceedence of the intergranular stresses by the shockwave, thereby causing the grain skeleton to deform. Because of the absence of porewater pressures the intergranular stresses during compaction are much higher for dry soils than for wet soils and the dynamic consolidation therefore less effective.

2 A ONE-DIMENSIONAL MODEL

2.1 Introduction

De Josselin de Jong (1956) describes some simple impact tests on dry sand samples. Identical cylindrical sand samples of 150 mm in height and 38 mm in diameter were subjected to impacts by small pounders. The impacts had a constant energy level but a varying duration. This variation was achieved by varying the height and cross-sectional area of the pounders. The resulting sample deformations gave evidence that the magnitude of the plastically deformed zone is proportional to the duration of the impact. This can be explained as follows.

In Figure 1 the idealised load-deformation behaviour of a dry granular soil under an axial load in a triaxial test

is given.

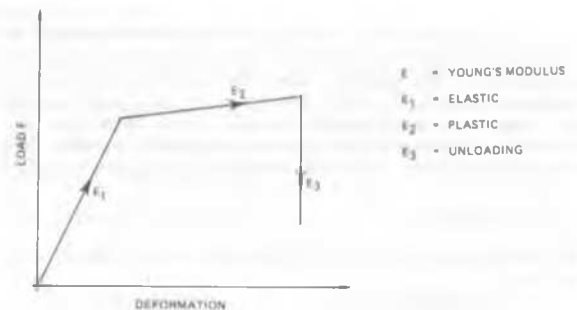


Figure 1. Load-deformation behaviour of a dry granular soil in a triaxial test

The wave front velocity for one-dimensional wave propagation is given by:

$$c = \sqrt{E/\rho} \quad (1)$$

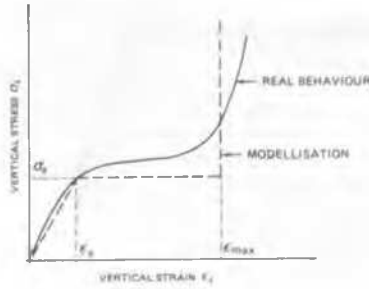
where c = wave front velocity (m/s)
 E = Young's modulus (N/m^2)
 ρ = density (kg/m^3)

Because the "Young's modulus" above the elastic limit E_2 is lower than the Young's modulus below the elastic limit E_1 , the velocity of the plastic wave front is considerably less than the velocity of the elastic wave front. During unloading, the soil reacts very stiff. The Young's modulus during unloading E_3 is higher than E_1 and E_2 . As a result of this, the unloading wave front travels faster through the soil sample than the plastic wave front, thus limiting the depth to which the plastic waves penetrate. If the period of the impact is lengthened, the plastic waves can penetrate to a greater depth which leads to higher resulting (plastic) deformations.

2.2 Soil model

If a loose granular soil is subjected to a sudden dynamic loading by a falling poulder above its elastic limit, it will deform plastically. The poulder has a tendency of punching through the soil and forcing a growing

cylindrical volume of soil downwards. Because of this punching mechanism the soil inside the cylindrical volume is forced into a state of confined compression. The vertical stress-strain behaviour of a loose granular soil under confined compression is as shown in Figure 2.



- ϵ_e - MAXIMUM ELASTIC AXIAL DEFORMATION
- ϵ_{max} - MAXIMUM TOTAL AXIAL DEFORMATION
- σ_e - ELASTIC LOAD LIMIT

Figure 2. Vertical stress-strain behaviour of a loose granular soil under confined compression

Upon initial loading, the grain skeleton deforms and the porosity decreases down to a certain lower limit. At this minimum porosity the soil has reached its maximum density and any further deformation can be achieved only by crushing of the grains. When the soil has reached its maximum density it will behave as a very stiff material. In Figure 2 the vertical stress-strain behaviour of a soil element underneath the poulder is given together with the simplified model used for example by Salvadori (1960).

2.3 The impact

If the poulder falls from a height h, the impact velocity v_0 is:

$$v_0 = \eta \sqrt{2gh} \tag{2}$$

where η - factor accounting for the loss of efficiency in the pounding cable system. (-)

From the moment of impact elastic waves will spread through the subsoil. If the impact exceeds the elastic limit of the soil σ_e , the vertical strains will first increase from 0 to ϵ_e and subsequently to ϵ_{max} (see Figure 2) From the moment the elastic limit σ_e is exceeded a compaction wave starts to propagate. If lateral spread of the cylindrical compacted zone is neglected, the situation is as shown in Figure 3.

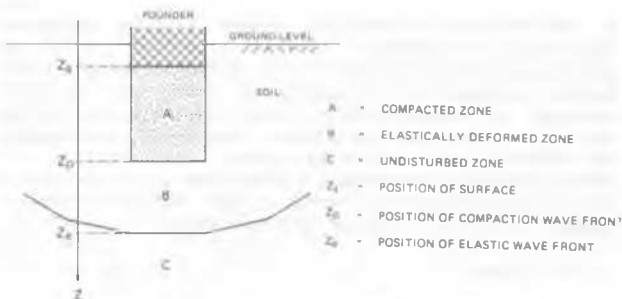


Figure 3. Soil deformations as a result of wave propagation

Since the soil inside the compacted zone is infinitely stiff, as defined in the schematized stress-strain relationship in Figure 2, it behaves as a rigid body. Both the rigid body and the poulder have to comply with the equation of motion.

The equation of motion for the poulder is:

$$F_s - m \frac{d^2 Z_s}{dt^2} \tag{3}$$

- where F_s - contact force between soil and poulder (N)
- m - mass of poulder (kg)
- Z_s - position of the soil surface (m)

In order to simplify the computations, consider only the displacements of the poulder after the elastic limit has been exceeded. The position of the soil surface relative to the elastic displacements, Z'_s , is given by:

$$Z'_s = Z_s - v_e t \tag{4}$$

where v_e - particle velocity in elastically deformed zone (m/s)

Substitution of (4) in (3) gives:

$$F_s - m \frac{d^2 Z'_s}{dt^2} \tag{5}$$

The equation of motion for the rigid body (the compacted zone) is:

$$-F_s - \sigma_e A - \rho_{max} A \frac{d}{dt} \left[(Z_p - Z_s) \frac{dZ'_s}{dt} \right] \tag{6}$$

- where σ_e - vertical stress at elasticity limit (N/m²)
- A - area of contact surface (m²)
- ρ_{max} - maximum soil density (kg/m³)
- Z_p - position of compaction wave front (m)

The position of the compaction wave front can be related to the position of the surface by implementing conservation of mass.

Conservation of mass requires, that

$$(Z_p - v_e t) \rho_e = (Z_p - Z_s) \rho_{max} \tag{7}$$

where ρ_e - soil density at elastic limit (kg/m³)

Substitution of (5) and (6) in (7) yields:

$$\frac{m}{A} \frac{d^2 Z'_s}{dt^2} + \sigma_e + \frac{\rho_{max} \rho_e}{\rho_{max} - \rho_e} \frac{d}{dt} \left[Z'_s \frac{dZ'_s}{dt} \right] = 0 \tag{8}$$

Solving differential equation (8) leads to an expression for Z'_s .

Compaction stops when $\frac{dZ'_s}{dt} = 0$, this is at a time T given by:

$$T = \frac{v_0 m}{A \sigma_e} \tag{9}$$

At this time T, the position of the compaction wave front is known and from this the depth H of the compacted zone can be derived:

$$H = Z_p - Z_s = \frac{m}{\rho_{max} A} \left[-1 + \sqrt{\frac{\sigma_e + \alpha v_0^2}{\sigma_e}} \right] \tag{10}$$

where α - density ratio, defined by:

$$\alpha = \frac{\rho_{max} \rho_e}{\rho_{max} - \rho_e} \tag{11}$$

Relations (10) and (11) indicate that the influence depth H of compaction is directly proportional to the ratio of poulder mass and base area and is also related to the 'elastic' and compacted soil densities. Because the elastic deformations are relatively small, this 'elastic' density is approximately the same as the in-situ density. Although approximate, equation (10) links the depth of the

compacted zone to the drop weight dimensions and soil conditions, i.e. it represents an improvement on the semi-empirical formulae of the form $H = m \cdot a \cdot b^D$ (h - drop height (m), m = weight of pounder in tonnes, a and $b \approx 0.5$) that are widely in use at present.

3 CASE STUDY

On a site in the eastern part of the Netherlands dynamic compaction was used as an alternative to a costly pile foundation. Dynamic compaction turned out to be more economical than other methods of deep densification such as blasting, grout injection, thermic treatment, vibro compaction, vibro replacement and compaction piles. The soil conditions varied between loose and dense sand with intermediate layers of loam. In Figure 4 some representative grainsize distributions of the upper soil layers are given. D_{50} varies between 0.18 and 0.25 mm, whereas the percentage of silt is approximately 10 %.

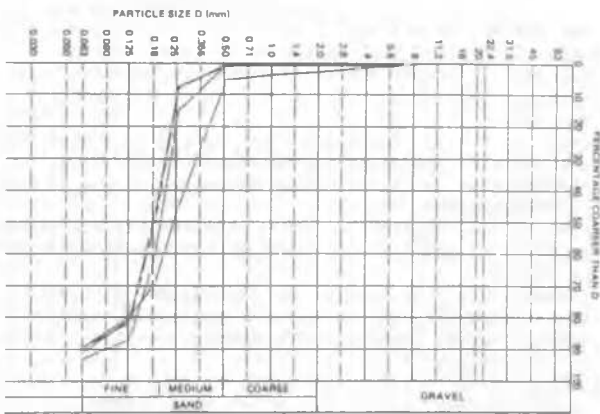


Figure 4. Representative grainsize distributions

The watertable was at approximately 30 meters below ground level.

The tamping pattern is shown in Figure 5.

The effect of the dynamic compaction process was checked by a number of Cone Penetration Tests (CPT's) made before and after compaction. In Figure 6 a representative example is given.

Interesting conclusions drawn from this case are:

- Compaction was concentrated immediately below the drop coverage. This was shown by a number of CPT's made at the impact points and between the impact points. No lateral spread of the compacted zone was observed, which confirms the previous assumptions to use a one-dimensional model.
- The one-dimensional model predicts a depth of the compacted zone of 6.3 m, assuming $\sigma_e = 250 \times 10^3 \text{ kN/m}^2$. σ_e was calculated by conventional static methods. The prediction by the approximate formula $H = \sqrt{(m \cdot h)}$ = 11.8 m largely overestimates the compaction depth.
- The increase in cone resistance was not as high as might have been expected from the empirical relationship of Baldi e.a. (1982) for normally consolidated sands. This effect is caused by the overconsolidation of the sand. The shock waves may have decreased the horizontal stresses in the soil thereby influencing the cone resistance.
- The average ground level settlement due to compaction was .33 metres. This decrease is in good agreement with an increase in soil density below the drop coverage from 1600 to 1800 kg/m³ over a depth of 6 m.
- Very pessimistic predictions of the future construction settlements were obtained using the results of the CPT's

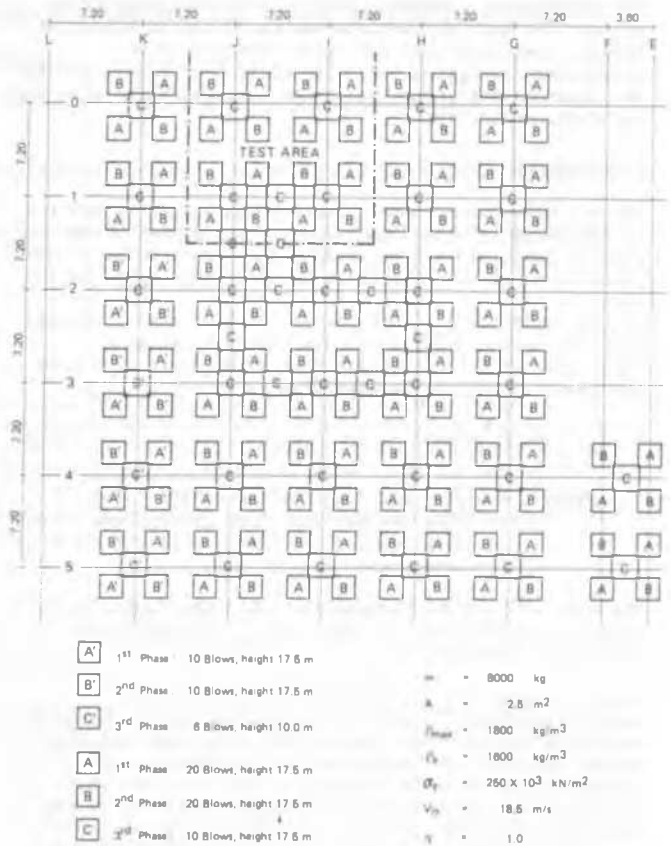


Figure 5. Tamping pattern

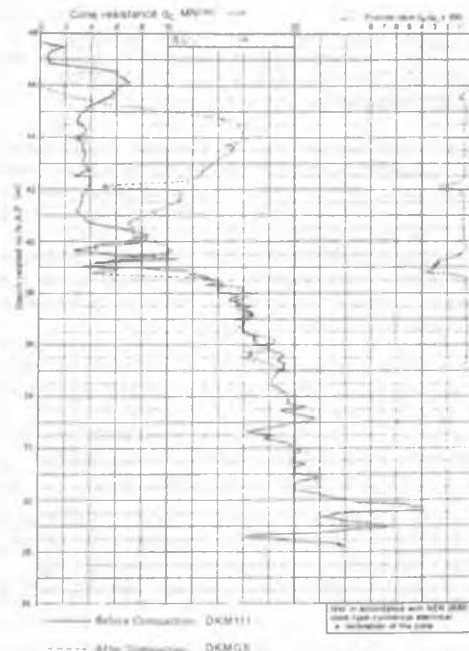


Figure 6. Cone penetration tests before and after compaction

and Schmertmann's method (1970). It is felt that CPT's are not the most appropriate way to check the effect of dynamic compaction and that more direct in situ measurement techniques, such as plate load tests, density measurements and plate load tests, are needed to give more accurate predictions.

4 VIBRATIONS

The one-dimensional model gives enough extra information on the period of the impact and the amplitude of the elastic displacements underneath the impact point to make predictions of the vibrations in the surroundings of the site.

If the amplitude u_{\max} and the period T of the vibrations near the impact point are known, the displacement amplitudes of soil particles at a large distance r from the impact point can be approximated by:

$$u(r) = \frac{u_{\max}}{\sqrt{r}} e^{-\alpha r} \quad (12)$$

where r - distance from the impact point (m)
 $u(r)$ - displacement amplitude at distance r (m)
 u_{\max} - displacement amplitude at impact point (m)
 α - attenuation factor (m^{-1})

The term $e^{-\alpha r}$ is the decrease in amplitude caused by material damping, whereas the term $\frac{1}{\sqrt{r}}$ represents the geometrical damping.

Dynamic compaction on dry granular soils is very unfavourable with respect to vibrations. Mainly Rayleigh waves are induced that have a low geometrical damping. Because of the low frequencies and the absence of porewater the material damping is also low. An other unfavourable effect of the low frequencies lies in the fact that they are close to the natural frequencies of many structures. Thus vibrations may be perceptible at distances of 1000 metres and more.

5 CONCLUSIONS

- The former case study has proven that dynamic compaction can be effective on dry granular soils. The influence depth of the compaction is less for dry granular soils than for saturated soils.

- The compaction mechanism in dry granular soils can be approximated reasonably well by a one-dimensional analytical model. In saturated soils, the one-dimensional model is not valid, because the compaction spreads over a larger area beneath the impact point. The one-dimensional model indicates that the influence depth of compaction is directly proportional to the ratio of poulder mass to base area and that it is also related to the in-situ and maximum soil densities.

- Settlements after compaction are overestimated when they are determined by using Schmertmann's method and the results of cone penetration tests only. Additional control measurements are necessary to check the effect of dynamic consolidation and to make better predictions of settlements after compaction.

- Because of the long period of the impact, low frequency vibrations in the surroundings are induced, which are close to the natural frequencies of many structures. The attenuation of these vibrations is very low for dry granular soils.

-The one-dimensional model provides enough extra information on the period of the impact and on the displacement amplitude underneath the impact point to make reliable

predictions of the vibrations at large distances from the impact point.

ACKNOWLEDGEMENTS

The authors would like to thank Mr. Meerman A. Lkol.gen., Advising Office Military Engineers of the Ministry of Defence of the Netherlands for his support of this study.

The authors are much indebted to Mr. H.J. Kolk of Fugro McClelland Engineers B.V. for reviewing this paper and providing helpful comments.

REFERENCES

- Baldi, G., Belotti, R., Ghionna, V., Jamiolkowski, M. and Pasqualini, E. (1982). Design parameters for sands from CPT. Proceedings of the 2nd European symposium on penetration testing, ESOPT II, Amsterdam, vol. 2, pp. 425-438, May 1982
- De Josselin de Jong, G. (1956). What happens in the soil during pile driving. (in Dutch). De Ingenieur no 25 pp. B77-88, June 1956
- Ménard, L. (1974). Application de la consolidation dynamique a l'amélioration des sols de fondation des ouvrages maritimes. K.V.I.V. 6th In 't Havenkongres, May 1974
- Ménard, L. (1974). Fondation d'une cale de Radoub à Brest sur terrain compressible preablement amélioré par la technique de la consolidation dynamique. K.V.I.V. 6th In 't Havenkongres, May 1974
- Ménard, L. and Broise, Y. (1975). Theoretical and practical aspects of dynamic consolidation. Géotechnique 25, no 1, pp. 3-18
- Salvadori, M.G., Skalak, R. and Weidlinger, P. (1960). Waves and shocks in locking and dissipative media. Journal of the Engineering Mechanics Division A.S.C.E. April 1960 pp. 77-105
- Schmertmann, J. (1970) Static cone to compute static settlement over sand. Journal of the Geotechnical Engineering Division A.S.C.E. Vol 96, SM 3 pp.1011-1043